

Infrared-induced dark states and coherent population trapping of excitons in quantum well structures

S. M. Sadeghi*

Department of Physics, University of Toronto, 60 St. George Street, Toronto, Canada M5S 1A7

W. Li[†]

Department of Chemistry and Engineering Physics, University of Wisconsin-Platteville, Platteville, Wisconsin 53818, USA, and Department of Electrical and Computer Engineering, University of Waterloo, Waterloo, Ontario, Canada N2L 3G1

(Received 1 June 2003; revised manuscript received 1 October 2003; published 22 January 2004)

We study enhancement of the $2s$ state emission intensity of the $e1$ - $hh1$ excitons via generation of dark states. This process is shown for a $\text{In}_{0.43}\text{Ga}_{0.57}\text{As}/\text{InP}$ quantum well structure interacting with a single infrared laser near resonance with the transition between $e1$ and $e2$. Via generation of strong nonparabolic hole dispersion, the tensile strain of this structure enhances the dipole moments of the nonallowed transitions between the $2s$ states of the $e1$ - $hh1$ and the $1s$ states of $e2$ - $hh1$ excitons. We show that, due to the simultaneous coupling of these transitions and those between the $1s$ states of the $e1$ - $hh1$ and $e2$ - $hh1$ excitons (allowed transitions), the infrared field can generate dark states, coherently pumping the $2s$ states of $e1$ - $hh1$ excitons and dramatically increasing their emission intensities. We also show that when the allowed and nonallowed transitions are driven by two resonant infrared field beams, coherent population trapping of excitons of the $e1$ - $hh1$ excitons occurs.

DOI: 10.1103/PhysRevB.69.045311

PACS number(s): 78.67.De, 78.60.-b, 78.55.Cr

I. INTRODUCTION

The $e1$ - $hh1$ excitons in quantum wells (QW's) have recently been used for prediction and testing of various novel applications. These applications include demonstration of photonic memory cell by prolonging the lifetimes of these excitons using an electric field,¹ implementation of quantum-information processes in quantum dots where the $e1$ - $hh1$ exciton states serve as qubits,² and ultrafast optical switching based on coherent control of spin and population of these excitons.³ The optical switching of the $e1$ - $hh1$ excitons has also been reported using intraband optical quantum-confined Stark effect. Here an intense infrared (IR) laser beam with polarization along the QW growth direction and frequency near resonant with the transition between the first ($e1$) and second ($e2$) conduction subbands was used to induce blue or red shift in the $e1$ - $hh1$ exciton emission,⁴ or absorption spectrum.⁵ This made the interband excitonic transitions of a QW nearly dark or transparent at the frequencies that it has, in the absence of the IR field, the maximum amount of emission intensity or absorption.

The previously studied intraband optical quantum confined Stark effects were mostly associated with mixing of the $e1$ - $hh1$ and $e2$ - $hh1$ exciton states with the same orbital angular moments (l) and principal quantum numbers (n). Here mostly the transitions between the s states of these excitons with the same principal quantum numbers (allowed transitions) were driven by an IR field, forming the so-called Ξ system [Fig. 1(a)]. Depending on the interface morphology and strain, however, interaction of an undoped QW structure with an IR field can be influenced by the dispersion of the hole subbands, making the coupling process different from a simple Ξ system. This is because, as discussed in Ref. 6 in details, the QW exciton states depend on the hole subband mixing or the degree of the nonparabolic dispersion of the valence subbands.⁷ Therefore for a range of tensile strains

this can lead to the enhancement of the dipole moments of the intersubband transitions between exciton states with different n 's (nonallowed transitions). Such transitions include those from $2s$ ($1s$) states of $e1$ - $hh1$ excitons to $1s$ ($2s$) states of the $e2$ - $hh1$ excitons.

Our objectives in this paper are to show how such a strain-induced enhancement of dipole moment can be used to create new optical systems in QW structures, to realize exciton dark states, and to find different ways to coherently control exciton emission and population. We discuss these issues by considering a tensile strained QW structure and show how its nonparabolic dispersion allows two-photon dressing of the $1s$ and $2s$ states of the $e1$ - $hh1$ excitons and coherent population trapping (CPT) of excitons. These phenomena are studied in a Λ_- system where the allowed and nonallowed transitions are driven by either one or two IR fields [Fig. 1(b)]. We show that when this system is created by two resonant IR laser beams, as that in Fig. 1(b), the CPT process equally distributes the $e1$ - $hh1$ population in two dark states,

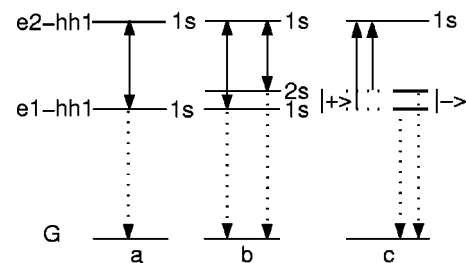


FIG. 1. Schematic diagrams of infrared coupling of a QW with a Ξ (a) and a Λ_- configuration (b). (c) represents the Λ_- system in the coherent basis. The vertical two-sided arrows refer to the intersubband excitonic couplings, the short horizontal dashed and solid lines represent, respectively, the bright ($|+\rangle$) and dark states ($|-\rangle$) at the $1s$ and $2s$ state energies of $e1$ - $hh1$ excitons, and the dashed arrows refer to the emission of the excitons.

one at the $1s$ and the other at the $2s$ state energies. As shown schematically in Fig. 1(c) (short solid lines), this leads to two illuminating lines at these energies. We also show that when the Λ_- system is generated by a single IR laser beam near resonant with the transition between the $2s$ states of e1-hh1 and $1s$ states of e2-hh1 it can coherently enhance the dim or even nonobservable photoluminescence of the $2s$ states. We attribute this effect to the dominant dark states generated by the single IR field leading to optical storage of the e1-hh1 excitons in the $2s$ states, making such dim states illuminating.

Note that the dark states studied in this paper are to some extent different from those discussed in the three-level atomic systems.⁸ In such systems usually the dark states were generated at the energies of the ground and a lower states. Therefore the transitions of a resonant probe field from these states to an upper state were prohibited. The systems discussed in this paper, however, consist of four levels and the dark states effectively suppress the intersubband transitions between the e1-hh1 and e2-hh1 states, as shown schematically in Fig. 1(c). Here, however, these states can undergo interband transitions by radiative decay. Additionally, one should note that the CPT discussed in this paper is different from that discussed in Ref. 9. In this reference the dark states were composed of excitons states associated with different conduction subbands, while in the present paper they are only composed of the e1-hh1 exciton states.

II. INFRARED-INDUCED COHERENT EFFECTS IN THE EXCITON EMISSION

The coherent effects studied in this paper are based on the formation of a Λ_- system [Fig. 1(b)]. This system is based on strain-induced enhancement of the dipole moments associated with the excitonic intersubband transitions. Here an IR laser with a polarization along the growth direction couples the $2s$ states of the e1-hh1 excitons with the $1s$ states of the e2-hh1 excitons while the same laser or a second laser mixes the $1s$ states of these excitons. As discussed in this paper, such a system could lead to two-photon dressing of the $1s$ and $2s$ states of the e1-hh1 excitons through the $1s$ states of e2-hh1 excitons, creating bright ($|+\rangle$) and/or dark ($|-\rangle$) states [Fig. 1(c)]. These states are given by

$$|-\rangle = \frac{[\Omega_{21}|\Psi_{e1}^{1s}\rangle - \Omega_{11}|\Psi_{e1}^{2s}\rangle]}{\mathbf{N}} \quad (1)$$

and

$$|+\rangle = \frac{[\Omega_{21}|\Psi_{e1}^{1s}\rangle + \Omega_{11}|\Psi_{e1}^{2s}\rangle]}{\mathbf{N}}. \quad (2)$$

Here $\mathbf{N} = \sqrt{\Omega_{11}^2 + \Omega_{21}^2}$, in which $\Omega_{11} = -\mu_{11}E_1/\hbar$ and $\Omega_{21} = -\mu_{21}E_2/\hbar$ are the Rabi frequencies associated with the transitions between the $1s$ states of the e1-hh1 and e2-hh1 excitons ($1s-1s$) and those between the $2s$ states of e1-hh1 and $1s$ states of e2-hh1 ($2s-1s$), respectively. E_1 and E_2 refer to the amplitudes of the IR fields and μ_{11} and μ_{21} are, respectively, the dipole moments associated with the $1s-1s$

and $2s-1s$ transitions. Ψ_{e1}^{ns} ($n=1$ and 2) refer to the exciton states associated with electrons in e1 and holes in hh1. Under the steady-state condition, due to destructive quantum interferences, the transitions between $|-\rangle$ and $|\Psi_{e2}^{1s}\rangle$ are suppressed, leading to accumulation of the e1-hh1 excitons in $|-\rangle$ and creation of CPT.

Our objectives in this paper are to study these issues and investigate how they can lead to CPT of e1-hh1 excitons and coherent enhancement of their $2s$ state emission. To proceed we consider the cases where the QW emission is caused by population of bound excitons, rather than by the Coulomb enhanced radiative decay of electron-hole pairs.¹⁰ This is possible when the excitons are generated resonantly or near resonantly at low temperatures and low densities.^{11,12} In addition, in this paper we consider QW structures such that their disorder-induced broadenings are less than the binding energies of their $2s$ excitons. This condition allows us to approximately separate center of motion and relative motion of the electrons and holes and consider the $1s$ and $2s$ exciton wave functions nearly unaffected by the disorder.^{13,14} The effective disorder potential, however, influences the center of mass of excitons causing localization, and homogeneous and inhomogeneous broadening of the emission linewidths. Furthermore, considering the small amount of disorder-induced broadening and relatively large energy spacing between $1s$ and $2s$ states, here we also ignore mixing of these states by the disorder potential.^{15,16} Note that a full quantitative treatment of these issues requires a detailed statistical analysis of the interface morphology, solving exciton motion in the presence of disorder potential including phonon scattering and radiative decay, and others.¹⁷ Such a treatment is beyond the scope of this paper, and therefore in the following we consider these effects in a phenomenological way.

Under the above mentioned conditions and the fact that under low excitation and low temperatures mainly the top hole subband (hh1) involves in the photoluminescence (PL) emission the state of an exciton can be presented as follows:

$$\Psi_i^{ns,\nu}(\mathbf{r}_e, \mathbf{r}_h) = \sum_{\mathbf{k}} G_i^{ns,\nu}(\mathbf{k}) e^{i\mathbf{k}\cdot(\rho_e - \rho_h)} C_i(z_e) v_{hh1,\mathbf{k}}^\nu(z_h) U U^\nu. \quad (3)$$

Here C_i is the electron wave function associated with the i th conduction subband and $v_{hh1,\mathbf{k}}^\nu$ refers to that of hh1 with spinor index ν . U and U^ν are the Bloch functions associated with electrons and holes, respectively. $G_i^{ns,\nu}(\mathbf{k})$ refer to the envelope functions of the excitons associated with hh1 spinor ν and electrons in the i th conduction subband. The exciton and hole envelope functions can be written as follows:¹⁸

$$G_i^{ns,\nu}(\mathbf{k}) = e^{j\nu\alpha} g_i^{ns,\nu}(k), \quad (4)$$

$$v_{hh1,\mathbf{k}}^\nu(z_h) = e^{-j\nu\alpha} v_{hh1,k}^\nu(z_h). \quad (5)$$

Here we have used $\mathbf{k} \equiv (k, \alpha)$. Note that since we only consider exciton s states with zero orbital angular momentum ($l=0$), instead of the z component of the total angular momentum of excitons, in the phase factor of Eq. (4) we only consider ν . Having this in mind and considering the interband selection rules of excitons that only allow involvement of $\nu = \mp 3/2$,¹⁸ we drop the index ν in the rest of this paper.

In addition, we ignore the Coulomb mixing between hh1 and other hole subbands, including the first light-hole subband (lh1). This is because inclusion of the Coulomb mixing effect does not change the physical processes discussed in this paper and may only cause coupling of exciton states with higher orbital angular momenta ($|l| > 1$). This means while the IR field mainly couples the s states, it may also cause, to lesser extent, coupling of the $2p$ states or the $3d$ states of excitons.

In QW structures with parabolic hh1 dispersion the principal quantum numbers of the initial and final states of the excitonic intersubband transitions (n and n') should be the same. In QW structures with nonparabolic hh1 dispersion, however, this restriction is relaxed.⁶ To see this and continue our development with the IR coupling of excitons, let us consider a system consisting of Ψ_{e1}^{ns} ($n=1$ and 2) and Ψ_{e2}^{1s} . Interaction of this system with two IR laser beams leads to the formation of a Λ_- system [Fig. 1(b)]. The Hamiltonian of such a system can be expressed as follows:

$$H^{\Lambda_-} = -\mu_{11}E_1(t)|\Psi_{e1}^{1s}\rangle\langle\Psi_{e2}^{1s}| - \mu_{21}E_2(t)|\Psi_{e1}^{2s}\rangle\langle\Psi_{e2}^{1s}| + \text{H.c.} \quad (6)$$

As mentioned above, $\mu_{nn'}$ refer to the dipole moments associated with the intersubband transitions in undoped QW's. In some literature they were considered independent of the excitonic effects, similar to those in n -doped QW's.¹⁹ As mentioned in the introduction, however, a consistent treatment shows that these moments depend strongly on excitonic features including spinor mixing of holes.⁶ To see this briefly note that the dipole moments of the intersubband transitions in undoped QW's are given by:

$$\mu_{nn'} = e\langle\Psi_{e1}^{ns}|z|\Psi_{e2}^{n's}\rangle. \quad (7)$$

Using Eqs. (3)–(5) and after imposing the excitonic interband and intersubband transition selection rules, $\mu_{nn'}$ for excitons in their radiative states are found as follows:

$$\mu_{nn'} = L \int k dk g_{e1}^{ns}(k) g_{e2}^{n's}(k) I(k). \quad (8)$$

Here L is the width of the QW and

$$I(k) = \int z dz C_{e1}(z) C_{e2}^*(z) v_{hh1,\mathbf{k}}(z) v_{hh1,\mathbf{k}}^*(z). \quad (9)$$

Inspection of Eqs. (8) and (9) shows that via excitonic effects the magnitudes of allowed ($n=n'$) and nonallowed ($n \neq n'$) intersubband transition dipole moments are strongly influenced by the hole dispersion. To see this note that the interband selection rules in narrow QW's only allow excitation of s states of e1-hh1 excitons. As a result, only heavy-hole components of the hh1 spinors ($\nu = \pm 3/2$) are involved in the interband transition process.¹⁸ Therefore, based on Eqs. (8) and (9), only when one considers parabolic dispersion for hh1 $\mu_{21}=0$ and μ_{11} is relatively large, similar to that associated with the transition between e1 and e2 without any excitonic effect. This issue can be understood considering the fact that for parabolic hh1 dispersion with no mixing effect the contributions of $\nu = \pm 3/2$ are the most and Eq. (9)

is independent of k . Under these conditions the orthogonality of the exciton wave functions associated with the $1s$ and $2s$ states in Eq. (8) requires $\mu_{21}=0$. However, when the nonparabolicity of hh1 is included and/or increased by strain the contributions of $\nu = \pm 3/2$ are decreased and those of $\nu = \pm 1/2$ are increased. Here $I(k)$ can become strongly k dependent making μ_{21} significant while suppressing μ_{11} .⁶ This issue will be seen quantitatively in the following section.

To find the emission spectra of the Λ_- system we used Eq. (6) to calculate the optical Bloch equations of this system. Under steady-state conditions, the solutions of these equations represented all components of the density matrix that described the states of the system. Using these components we then applied linear response theory to calculate the emission spectra of the QW for the interband transitions.

III. COHERENT POPULATION TRAPPING OF $1s$ AND $2s$ STATES OF E1-HH1 EXCITONS

The formalism developed in the preceding section can be applied to various structures, including GaAs/AlGaAs, GaAsP/AlGaAs, InGaAs/InP and others. However, as mentioned above, within the approximations considered in this paper, the interface roughness and alloy inhomogeneity of these structures should be small enough such that their effects on the wave functions of the $1s$ and $2s$ states can be neglected. Having this in mind, here we consider a single 6-nm $\text{In}_{0.43}\text{Ga}_{0.57}\text{As}$ QW confined by InP barriers. Although growth of such a structure usually deals with alloy fluctuations, there are some studies showing that the PL broadening caused by such a disorder can become as low as 1.3 meV.²⁰ In addition, since using state-of-art growth systems,²⁰ growth interruption,²¹ or QW thickness adjustment²² one can expect smooth interfaces, in the following we assume the emission linewidth of this structure is around 1.5 meV. Such a linewidth is less than the binding energies of $1s$ and $2s$ excitons in this structure that are considered to be ~ 8 and ~ 2 meV, respectively.²³

The conduction band of the QW structure considered in this paper supports two subbands (e1 and e2) with ~ 137 meV energy spacing and its valence band has several hh and lh subbands. In addition, because of 0.7% tensile strain the hh1 subband of the QW structure considered in this paper is strongly nonparabolic, as can be seen in Fig. 2. Also since we consider low temperatures, due to the disorder the excitons are mainly localized,²⁴ although with small amount of Stokes shift. We assume the homogeneously broadened linewidths of the $1s$ and $2s$ states of the e1-hh1 excitons are 0.3 and 0.7 meV, respectively. The latter includes the energy relaxation of $2s$ states into the $1s$ states via emission of acoustic phonons with a time scale of 10 ps. In addition, we consider the ratio of the oscillator strengths of the $2s$ to $1s$ states to be $1/7$. Note, however, that since the $2s$ states have larger Bohr radius than those of the $1s$ states, their wave functions average over a larger region in the plane of the QW. Therefore, the strength of the disorder potential experienced by the $2s$ states can be less than that experienced by the $1s$ states. This may make this ratio larger compared to those in the case of free excitons.¹⁶ In addition, application

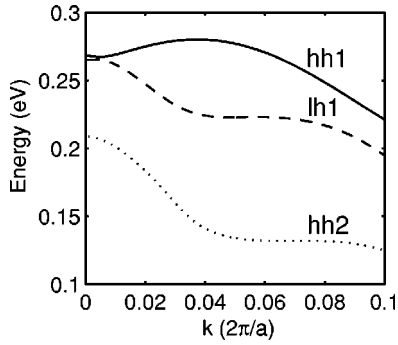


FIG. 2. Valence band structure of the QW structure studied in this paper. The solid, dashed, and dotted lines refer to the hh1, lh1, and hh2, respectively. The energies are presented from the edge of the valence band.

of the formalism developed in the preceding section to the QW structure considered in this paper showed that $\mu_{11} \sim 8.5e \times \text{\AA}$ and $\mu_{21} \sim 2e \times \text{\AA}$. Note that the enhancement of μ_{21} comes with the cost of suppression of μ_{11} . This is related to that the fact under 7% tensile strain the contribution of $\nu=3/2$ in hh1 is reduced and replaced by that of $\nu = -1/2$.⁶

Because of its band structure (Fig. 2), there are three possible emission processes for e1-hh1 excitons in the QW structure considered in this paper. These processes are (a) phonon-assisted transitions, (b) indirect transitions with no phonon replica, and (c) direct transitions. Amongst these three, at low temperatures and low excitation, the indirect transitions (b) are the most dominant ones. As discussed in Refs. 25 and 26, this process is caused by the uncertainty of the exciton wave vector \mathbf{K} caused by disorder. In fact at low temperatures mainly due to alloy fluctuations, localization in InGaAs/InP is strong.²⁴ Because of this, the exciton wave vector becomes uncertain,^{27,28} allowing finite probabilities for the excitonic transitions at $\mathbf{K} \sim \mathbf{0}$. Note that this uncertainty can influence the line shape of PL emission causing a long energy tail.²⁸ In this paper since we consider low temperature and small disorder, we adopt Gaussian line shapes for the PL emission.

Coherent processes discussed in this paper are strongly influenced by the characteristics dephasing rates of the excitonic intersubband transitions. Since we consider the density of photoexcited carriers is low, these rates are dominated by the scattering of excitons with phonons and with the potential fluctuations caused by the disorder. The phonon-e1-hh1 exciton scattering is mainly dominated by that with acoustic phonons while the e2-hh1 excitons are mostly scattered with longitudinal optical (LO) phonons. The latter leads to ionization of the e2-hh1 excitons, causing electrons with large wave vectors in e1 and holes in hh1. Since these electrons cannot constitute bound states with the holes before they undergo momentum and energy relaxation, this process increases the chance of their nonradiative recombination with holes and decreases the quantum efficiency of the e1-hh1 exciton emission. This effect that has been experimentally and theoretically investigated in Refs. 4 and 7 is quantitatively represented by a loss rate in this paper. In practice this

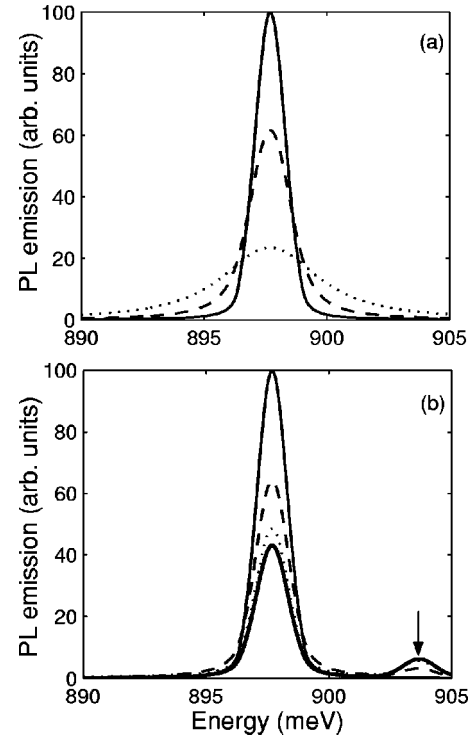


FIG. 3. PL emission of the QW with a Ξ (a) and a Λ_- configuration (b). In (a) the solid, dashed, and dotted lines refer to $\Omega_{11} = 0, 0.5$ and 1 ps^{-1} , respectively, and in (b) to $\Omega_{11} = \Omega_{21} = 0, 0.5$, and 1 ps^{-1} . The thick solid line refers to $\Omega_{11} = \Omega_{21} = 5 \text{ ps}^{-1}$.

rate depends on the sample quality. Here we assume this to be 0.01 ps^{-1} . The rate of the e2-hh1-LO-phonon scattering is considered to be 5 ps^{-1} . In addition, we also assume that in the absence of the IR laser the $2s$ -state population of the e1-hh1 excitons is insignificant. This implies that the electron-hole pairs that are generated either by the interband pump field or by ionization of the e2-hh1 excitons are mostly transferred into the $1s$ states of e1-hh1. This is in accordance with the fact that the $2s$ states of e1-hh1 excitons are dim and the ratio of their PL emission intensities to those of the $1s$ states has been found to be as low as $1/200$.^{29,30}

To study CPT of e1-hh1 excitons we need an efficient two-photon dressing between their $1s$ and $2s$ states. Therefore here we consider two IR fields, one resonant with the $1s$ - $1s$ and the other with the $2s$ - $1s$ transitions forming a resonant Λ_- system [Fig. 1(b)]. This system allows us to independently adjust the intensities of the two fields such that their Rabi frequencies become the same, $\Omega_{21} = \Omega_{11}$, creating a balanced two-photon coupling process. Considering the magnitudes of μ_{11} and μ_{21} , one can relate these frequencies to the intensities of IR fields as $I_{11} = 0.33 \times \Omega_{11}^2$ and $I_{21} = 6 \times \Omega_{21}^2$.

Before addressing CPT in the e1-hh1 exciton emission, it is useful to first study the emission of a resonant Ξ system [Fig. 1(a)] by turning off the field resonant with the $2s$ - $1s$ transition in Fig. 1(b) and assuming $\mu_{21} = 0$. As shown in Fig. 3(a), here as Ω_{11} increases the emission spectrum associated with the $1s$ states of the e1-hh1 quenches and broadens drastically. This is in accordance with the fact that the

intraband excitonic transition enhances the nonradiative decay rates of the e1-hh1 excitons⁷ and the linewidth of these excitons increases due to their IR mixing with the broad 1s states of e2-hh1 excitons. For higher field intensities the spectrum might show some sign of the Autler-Townes doublet caused by the IR dressing of the 1s states of e1-hh1 and e2-hh1 excitons. Observation of this effect depends on the sample loss rate and the linewidths of the Ψ_{e1}^{1s} and Ψ_{e2}^{1s} . The narrower (broader) is the former (the latter), the less probable is the observation of this effect. In the QW structure considered in this paper the doubling effect is found to be insignificant.

When one considers a resonant Λ_- system, in which the 1s-1s and 2s-1s transitions are strongly driven by two IR fields, the results are drastically different from those of the Ξ system. Here, as Fig. 3(b) shows, the e1-hh1 emission undergoes a peculiar quenching without any sign of significant broadening. This process rapidly reaches a saturation limit where the dynamic of the system is frozen and the intense IR fields can no longer change the emission spectrum. In addition, the resonant Λ_- system generates another emission peak (shown by an arrow) at the energies of the 2s states of the e1-hh1 excitons. Similar to the main peak, the intensity of this peak also reaches a saturation limit where any increase of the IR field intensities becomes ineffective.

To discuss the results seen in Fig. 3, note that in the resonant Λ_- system a broad state (Ψ_{e2}^{1s}) was coupled to two relatively narrow states (Ψ_{e1}^{1s} and Ψ_{e1}^{2s}). As a result, the narrow states were effectively dressed via two-photon coupling, generating $|+\rangle$ and $|-\rangle$ [Fig. 1(c)]. However, since we considered the IR fields were either continuous wave (cw) or in pulsed form with temporal widths much longer than the characteristic dephasing times of the excitonic intersubband transitions, the system evolved into steady state where $|+\rangle$'s were annihilated and two stable dark states, one at the energy of 1s states ($|-\rangle_{1s}$) and another at that of 2s states ($|-\rangle_{2s}$) were established. These processes led to CPT of the e1-hh1 excitons. Under this condition the e1-hh1 excitons became immune against the nonradiative decay enhancement caused by the one-photon 1s-1s and 2s-1s transitions and the system dynamic was frozen.

Note that when CPT occurs the e1-hh1 excitons are equally distributed between $|-\rangle_{1s}$ and $|-\rangle_{2s}$ [Fig. 1(c)]. This is the reason of the peculiar quenching seen in the main peak of Fig. 3(b) and creation of the extra emission peak at higher energy. Using Eq. (1) and a dressed photon-exciton picture one can show that the main emission peak is caused by the decay of the 1s-state components of the $|-\rangle_{1s}$ (Ψ_{e1}^{1s}) while the extra peak is generated by the emission of the 2s state components of $|-\rangle_{2s}$ (Ψ_{e1}^{2s}).³¹ The emission intensities of these states are renormalized by their radiative oscillator strengths while their populations are the same.

IV. COHERENT ENHANCEMENT OF EMISSION INTENSITY OF DIM EXCITONS

The PL emissions of the 2s states of the e1-hh1 excitons are usually dim or hardly observable. This is mainly because

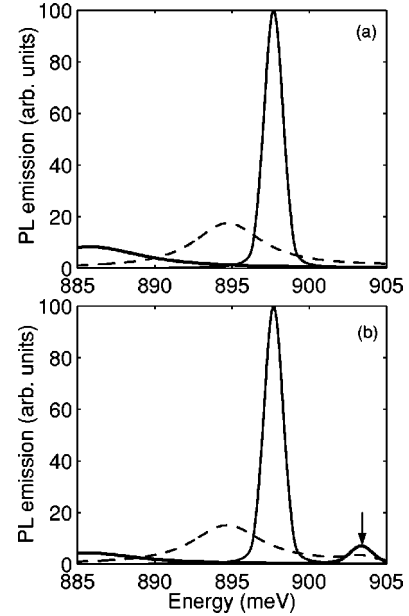


FIG. 4. PL emission of the QW with a detuned Ξ (a), and a detuned Λ_- (b) configuration generated by a single infrared field. The solid, dashed, and thick solid lines refer to 0, 1, and 5 MW/cm² field intensities, respectively.

(i) the energy relaxation rates of the electron-hole pairs into these states are smaller than those into the 1s states,²⁹ (ii) the 2s states decay into 1s states via emission of acoustic phonons, and (iii) since they have small binding energies, they can be easily ionized thermally. In the preceding section we showed that by creating CPT one can increase the emission intensity of these states. In that case the e1-hh1 population was equally distributed between dark states with optically active 1s state ($|-\rangle_{1s}$) and 2s state ($|-\rangle_{2s}$). In this section we show how the strain-induced enhancement of intersubband transition dipole moments and coherent effects allow one to enhance the emission intensity of the 2s states using a single IR field. This is done by effectively populating $|-\rangle_{2s}$ while $|-\rangle_{1s}$ has much less population.

To study enhancement of the 2s state emission here we consider interaction of the QW structure described in the preceding section with a single IR laser beam. This laser is polarized along the growth direction and its photon energy is ~ 1 meV less than that of the 2s-1s transition. To proceed we first assume $\mu_{21} = 0$. Although this assumption is unrealistic for the present structure it has the advantage of clarifying our discussion and presents optical quantum-confined stark effect in structures that have parabolic or nearly parabolic hh1 subbands.⁴ As Fig. 4(a) shows, under these conditions the emission peak is broadened and quenched while it is shifted to lower energies. This phenomenon has been experimentally tested in GaAs/AlGaAs QW structure and attributed to the two-level coupling of the e1-hh1 and e2-hh1 exciton states [Ξ system, Fig. 1(a)].⁴ The situation is different when we consider the effects of μ_{21} . Here under similar conditions as those in Fig. 4(a), in addition to the optical red shifting of the main emission peak, the 2s states of the e1-hh1 excitons become illuminating. As shown in Fig. 4(b), the

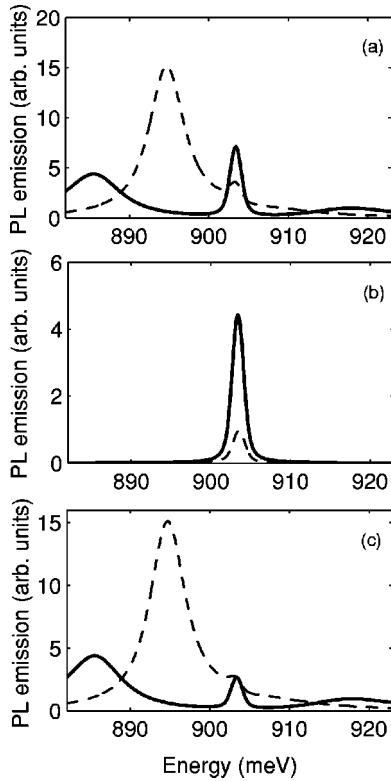


FIG. 5. Contributions of the $2s$ (b) and $1s$ (c) emission spectra to the total PL emission (a) of the QW with a detuned Λ_- configuration caused by a single infrared field. Dashed and thick solid lines refer to 1 and 5 MW/cm^2 intensities, respectively.

emission peak of these states (shown by an arrow) reaches a saturation limit at relatively low-field intensities while further increase of the IR field intensity reduces the amplitude of the red-shifted peak as it is additionally shifted to lower energies.

The results seen in Fig. 4(b) happened despite the fact that we did not assume any energy relaxation of electron-hole pairs into the $2s$ states of the e1-hh1 excitons. This suggests that the emission enhancement of the $2s$ states is solely caused by the detuned Λ_- system created by the single IR field. To clarify this issue and find out the role played by the dark states and other coherent processes, note that the emission spectra seen in Fig. 4(b) are the results of superposition of emission spectra of two sets of dressed states. These sets are caused by one- and two-photon couplings of the $1s$ and $2s$ states of e1-hh1 with the $2s$ states of e2-hh1. The two-photon coupling leads to the generation of $|-\rangle_{1s}$ and $|-\rangle_{2s}$, and the one-photon coupling process mixes the $1s$ and $2s$ states of e1-hh1 with the $2s$ states of e2-hh1. Similar to the two-photon states, in one-photon states also either $1s$ or $2s$ states can decay radiatively via interband transition.³²

Having this in mind we investigate the evolutions seen in Fig. 4(b) by separating the contributions of each of these sets of dressed states. This is done by putting the oscillator strengths associated with the decay of the $1s$ or $2s$ states equal to zero by hand. As Fig. 5(b) shows, the contributions of the $2s$ state emission when the IR field intensity is 1 (dashed line) or 5 MW/cm^2 (solid line) are mainly single

emission peaks at the $2s$ state energies. This phenomenon suggests that the evolution of these states are mainly determined by $|-\rangle_{2s}$. On the other hand, as shown in Fig. 5(c), the contributions of the $1s$ states are mainly composed of relatively weak central peaks at the $2s$ state energies and creation of two sidebands. The energies of the central peaks do not change as the field intensity increases, but the sidebands are pushed away from each other. This suggests that the central peaks are associated with $|-\rangle_{1s}$. The sideband peaks, however, are originated by the dressed states caused by the one-photon coupling of $1s$ and $2s$ states of e1-hh1 and e2-hh1 states.³² In these dressed states only the $1s$ states can decay radiatively. Figure 5(a) shows the summations of the corresponding contributions in Figs. 5(b) and 5(c), which are identical to the corresponding ones shown in Fig. 4(b).

The results seen in Fig. 5 show that the enhancement of $2s$ state emission caused by a single IR field is different from that seen in the case of CPT. The latter was caused by two IR fields with the same Rabi frequencies ($\Omega_{11} = \Omega_{21}$). This led to an effective resonant two-photon coupling and creation of dark states with equal populations. This process was accompanied by strong suppression of the one-photon coupling process. In the case of Figs. 4(b), however, since a single IR field was used and $\mu_{21}/\mu_{11} \sim 0.2$, the Rabi frequency associated with the $1s$ - $1s$ was much larger than that of the $2s$ - $1s$ transition. Therefore, although the IR field was nearly resonant with the $2s$ - $1s$ transition and well detuned from the $1s$ - $1s$ transition, the one-photon coupling with sideband manifestation played the main role in the emission of the $1s$ states. As a result, here the emission of the $1s$ states nearly followed the evolution of a detuned Ξ system, similar to that Fig. 4(a). On the other hand, because of the detuned two-photon process the population of $|-\rangle_{1s}$ became much smaller than that of $|-\rangle_{2s}$.

V. CONCLUSIONS

In conclusion, we studied coherent enhancement of the emission intensity of $2s$ states of the e1-hh1 excitons via asymmetric dressing of these states with the $1s$ states of the same excitons. Such a dressing process was generated by a single IR laser near resonance with the transition between the first and second conduction subbands of a tensile strained QW structure. The tensile strain enhanced the dipole moment associated with the transitions between the $2s$ states of e1-hh1 and the $1s$ states of e2-hh1. As a result, these transitions and those between $1s$ states of e1-hh1 and e2-hh1 were simultaneously driven by a single IR field. We also showed that when the QW interact with two IR fields, this system could lead to coherent population trapping of the e1-hh1 excitons as two dark states were generated at the $1s$ and $2s$ energies of e1-hh1. Although the intersubband transitions from these states into an upper subband were inhibited, they could radiatively decay into the QW ground state forming two emission lines.

ACKNOWLEDGMENTS

This research was supported by the Natural Sciences and Engineering Research Council of Canada and Photonic Research Ontario.

- *Present address: Photonami Inc., 50 Mural Street, Richmond Hill, Ontario, Canada L4B 1E4. Electronic address: sm.sadeghi@utoronto.ca
- †Present address: Department of Chemistry and Engineering Physics, University of Wisconsin-Platteville, Platteville, WI 53818, USA.
- ¹S. Zimmermann, A. Wixforth, J.P. Kotthaus, W. Wegscheider, and M. Bichler, *Science* **283**, 1292 (1999).
 - ²F. Troiani, U. Hohenester, and E. Molinari, *Phys. Rev. B* **62**, 2263 (2000).
 - ³A.P. Heberle, J.J. Baumberg, T. Kuhn, K. Kohler, and K.H. Ploog, *IEEE J. Sel. Top. Quantum Electron.* **2**, 796 (1996).
 - ⁴S.M. Sadeghi and J. Meyer, *J. Phys.: Condens. Matter* **12**, 5801 (2000).
 - ⁵D. Frohlich, R. Wille, W. Schlapp, and G. Weimann, *Phys. Rev. Lett.* **59**, 1748 (1987).
 - ⁶S. M. Sadeghi and W. Li (unpublished).
 - ⁷S.M. Sadeghi, J. Meyer, T. Tiedje, and M. Beaudoin, *IEEE J. Quantum Electron.* **36**, 1267 (2000).
 - ⁸M. Scully and M. Zubiary, *Quantum Optics* (Cambridge University Press, Cambridge, England, 1997).
 - ⁹S.M. Sadeghi and H.M. van Driel, *Phys. Rev. B* **63**, 045316 (2001).
 - ¹⁰M. Kira, F. Jahnke, and S.W. Koch, *Phys. Rev. B* **81**, 3263 (1998).
 - ¹¹D. Hagele, J. Hubner, W.W. Ruhle, and M. Oestreich, *Physica B* **271**, 328 (1999).
 - ¹²W. Hoyer, M. Kira, and S.W. Koch, *Phys. Rev. B* **67**, 155113 (2003).
 - ¹³R. Zimmermann, F. Große, and R. Runge, *Pure Appl. Chem.* **69**, 1179 (1997).
 - ¹⁴R. Zimmermann and R. Runge, in *Proceedings of the 22nd International Conference on the Physics of Semiconductors* (World Scientific, Singapore, 1994), p. 1424.
 - ¹⁵G. Bastard, C. Delalande, M.H. Meynadier, P.M. Frijlink, and M. Voos, *Phys. Rev. B* **29**, 7042 (1984).
 - ¹⁶S. Jaziri and R. Ferreira, *Phys. Status Solidi B* **221**, 337 (2000).
 - ¹⁷R. Zimmermann and R. Runge, *Phys. Status Solidi A* **164**, 511 (1997).
 - ¹⁸L.C. Andreani and A. Pasquarello, *Phys. Rev. B* **42**, 8928 (1990).
 - ¹⁹W.J. Li, B.D. McCombe, F.A. Chambers, G.P. Devane, J. Ralston, and G. Wicks, *Phys. Rev. B* **42**, 11 953 (1990).
 - ²⁰W.T. Tsang and E.F. Schubert, *Appl. Phys. Lett.* **49**, 220 (1986).
 - ²¹I. Yamakawa, T. Yamauchi, R. Oga, Y. Fujiwara, Y. Takeda, and A. Nakamura, *Jpn. J. Appl. Phys.* **42**, 1548 (2003).
 - ²²D.C. Bertolet, J.-K. Kuei, K.M. Lau, E.S. Koteles, and D. Owens, *J. Appl. Phys.* **64**, 6562 (1988).
 - ²³J. Shao, D. Haase, A. Dornen, V. Harle, and F. Scholz, *J. Appl. Phys.* **87**, 4303 (2000).
 - ²⁴J. Hegarty, K. Tai, and W.T. Tsang, *Phys. Rev. B* **38**, 7843 (1988).
 - ²⁵V. Harle, H. Bolay, E. Lux, P. Michler, A. Moritz, T. Forner, A. Hangleiter, and F. Scholz, *J. Appl. Phys.* **75**, 5067 (1999).
 - ²⁶P. Michler, A. Hangleiter, A. Moritz, G. Fuchs, V. Harle, and F. Scholz, *Phys. Rev. B* **48**, 11 991 (1993).
 - ²⁷K. Leosson, J.R. Jensen, W. Langbein, and J.M. Hvam, *Phys. Rev. B* **61**, 10 322 (2000).
 - ²⁸R.F. Schnabel, R. Zimmermann, D. Bimberg, H. Nickel, R. Losch, and W. Schlapp, *Phys. Rev. B* **46**, 9873 (1992).
 - ²⁹P. Dawson, P. Buckle, M.J. Godfrey, W.H. Roepke, and M. Hall-sall, *Solid State Commun.* **101**, 477 (1997).
 - ³⁰K.J. Moore, P. Dawson, and C.T. Foxon, *Phys. Rev. B* **34**, 6022 (1986).
 - ³¹C. Cohen-Tannoudji, J. Dupont-Roc, and G. Grynberg, *Atom-Photon Interactions* (Wiley, New York, 1999).
 - ³²S.M. Sadeghi, J.F. Young, and J. Meyer, *Phys. Rev. B* **56**, R15 557 (1997).